Available online at www.sciencedirect.com

SciVerse ScienceDirect

Ceramics International 39 (2013) 3547–3554

CERAMICS INTERNATIONAL

www.elsevier.com/locate/ceramint

Influence of pressure on filtration of aqueous alumina suspensions

Yoshihiro Hirata[a,*], Tomoyuki Fukunaga[a], Naoki Matsunaga[b], Soichiro Sameshima[a]

[a]*Department of Chemistry, Biotechnology, and Chemical Engineering, Kagoshima University, 1–21-40 Korimoto, Kagoshima 890-0065, Japan*
[b]*Department of Environmental Robotics, University of Miyazaki, 1-1 Gakuen- Kibanadai nishi, Miyazaki 889–2192, Japan*

Received 9 October 2012; accepted 9 October 2012
Available online 16 October 2012

Abstract

The dispersibility of colloidal alumina particles (median size 310 nm) was related to the surface potential, the solid concentration in a suspension and the pressure applied to the particles. The consolidation behavior of colloidal alumina particles with an isoelectric point pH 8.7 was examined using a developed pressure filtration apparatus at 1–10 MPa of applied pressure. The height of 7 or 20 vol% alumina suspensions at pH 3.0, 7.8 and 9.0 as a function of filtration time was fitted by a filtration model developed for a flocculated suspension rather than a traditional filtration model for a dispersed suspension. An increased pressure, a decrease of particle concentration and a porous microstructure of colloidal cake reduced the consolidation time of alumina suspension. The wet alumina compacts were significantly compressed during filtration but relaxed after the release of the applied pressure. However, the packing density of alumina compact after calcination at 700 °C was almost independent of the filtration pressure and controlled by the structure of network of alumina particles in a solution.

Keywords: A. Slip casting; B. Porosity; D. Al_2O_3

1. Introduction

Pressure filtration can shorten the consolidation time of colloidal suspensions of nanometer-sized or submicrometer-sized particles and produce dense compacts [1–4]. The applied pressure of pressure filtration can be as high as 80 MPa when stainless steel equipment is used [1]. However, the filtration process of ceramic particles at a high pressure has been scarcely analyzed. In past seven years, our group analyzed the consolidation behavior of aqueous suspensions of hydroxyapatite, silicon carbide, 8 mol% yttria–stabilized zirconia, and alpha-alumina powders in a size range from 20 to 800 nm using a newly-developed pressure filtration apparatus up to 19 MPa [5]. From the relation between applied pressure (ΔP_t) and volume of dehydrated filtrate (V_f), it was found that a phase transition from a dispersed state to a flocculated state occurs at a critical applied pressure (ΔP_{tc}). The phase transition pressure at a constant crosshead speed of piston is affected by particle concentration, particle size, surface potential, degree of dissociation of polyelectrolyte dispersant and applied electric field [6,7]. The influence of above factors was discussed theoretically and experimentally in our previous paper [7]. The ΔP_{tc} increases in the following conditions: (1) an increase of particle concentration for the condition that chemical potential of dispersed particles is greatly increased by the increased concentration, (2) an increase of particle size, and (3) an increase of surface potential. The steric or electrosteric stabilization of colloidal particles by excess polyelectrolyte leads to the increased ΔP_{tc}. Application of a direct current field during pressure filtration provides a temporary increase of applied pressure as a function of amount of filtrate [8]. In contrast to DC field, AC field accelerates the flocculation of charged particles and leads to the decreased applied pressure during filtration [9]. In our previous papers [10,11], the consolidation behavior of colloidal SiC particles (30 nm diameter) at a constant pressure was also analyzed based on the filtration model for a flocculated suspension. The purpose of this paper is to clarify the consolidation behavior of 300 nm alumina particles in a wide pH range of pH 3.0–9.0 during pressure filtration at 1–10 MPa of applied pressure. The packing density and microstructure of the consolidated

*Corresponding author. Tel.: +81 99 285 8325; fax: +81 99 257 4742.
E-mail address: hirata@apc.kagoshima-u.ac.jp (Y. Hirata).

0272-8842/$ - see front matter © 2012 Elsevier Ltd and Techna Group S.r.l. All rights reserved.
http://dx.doi.org/10.1016/j.ceramint.2012.10.180

alumina compact are issues of scientific interest. In this paper, the influence of suspension pH and applied pressure on the consolidation of colloidal alumina particles is discussed.

2. Experimental procedure

A high purity alpha-alumina powder with an isoelectric point pH 8.7 ($Al_2O_3 > 99.99$ mass%, specific surface area 10.5 m^2/g, Sumitomo Chemical Co. Ltd. Tokyo, Japan) was dispersed in double distilled water to make 7 or 20 vol% solid suspensions at pH 3.0, 7.8 and 9.0, respectively. The particle size distribution in a dilute alumina suspension at pH 3.0 was measured by a particle size distribution analyzer (Particle Size Distribution Analyzer CAPA–700, Horiba, Tokyo, Japan) and the particle sizes at cumulative 10, 50 and 90% were 210, 310 and 580 nm, respectively (Fig. 1(a)). Fig. 1(b) shows a transmission electron micrograph image of alumina particles. The primary particles have elongated morphology. The zeta potential of alumina particles was measured at a constant ionic strength of 0.001 M-NH_4NO_3 solution (Rank Mark II, Rank Brothers Ltd, Cambridge, UK). The shear stress–shear rate relations of 7–20 vol% alumina suspensions were measured by a cone and plate viscometer at 25 °C (Brookfield, DV-II+Pro Viscometer, UK). The alumina suspensions were consolidated through a glass filter with a 20 μm pore diameter and three sheets of a membrane filter with a 0.1 μm pore diameter, which were attached to the bottom of the piston (polymeric resin) moving at a constant pressure (1–10 MPa). The schematic structure of the pressure filtration apparatus is presented in Ref. 11. The applied load and the height of piston were continuously recorded (Tensilon RTC–1350 A, A&D Co., Ltd, Tokyo, Japan). The consolidated alumina compacts were taken out of the cylinder and dried at 100 °C in air for 24 h. The dried compacts were heated at 700 °C in air for 1 h to give an enough strength for the measurement of bulk density by the Archimedes method using double distilled water. Little difference of bulk densities was observed between a calcined compact (measured by the Archimedes method) and a dried compact (measured by its weight and geometrical sizes) owing to the low calcination temperature. The microstructures of calcined compacts were observed by a scanning electron microscope (SM-300, Topcon Co., Tokyo, Japan).

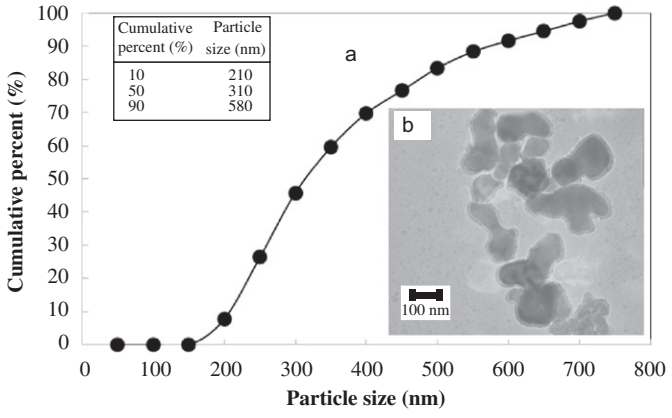

Fig. 1. (a) Particle size distribution of as-received alumina particles and (b) transmission electron micrograph of primary particles.

3. Filtration models

The filtration theories of dispersed and flocculated suspensions were reported in our previous papers [5–7,10]. A filtration process for well dispersed particles, shown in Fig. 2(a), was analyzed by Aksay and Schilling [2]. The relation of piston height (h_t)–filtration time (t)–applied pressure ($\Delta P_t = P_t - P_0$) in Fig. 2(b) is approximated by Eq. (1),

$$\Delta P_t t = \frac{\eta \alpha_c}{2n}(H_0 - h_t)^2 \quad (1)$$

where η is the viscosity of filtrate, α_c is the specific resistance of porous consolidated layer, H_0 is the initial suspension height, n is the system parameter ($\equiv(1-C_0-\varepsilon_c)/C_0$, ε_c is the volume fraction of voids in the consolidated layer, C_0 is the initial particle concentration).

A phase transition from a dispersed suspension to a flocculated suspension occurs at a critical applied pressure (ΔP_{tc}) [5]. Fig. 2(c) and (d) show a schematic structure of

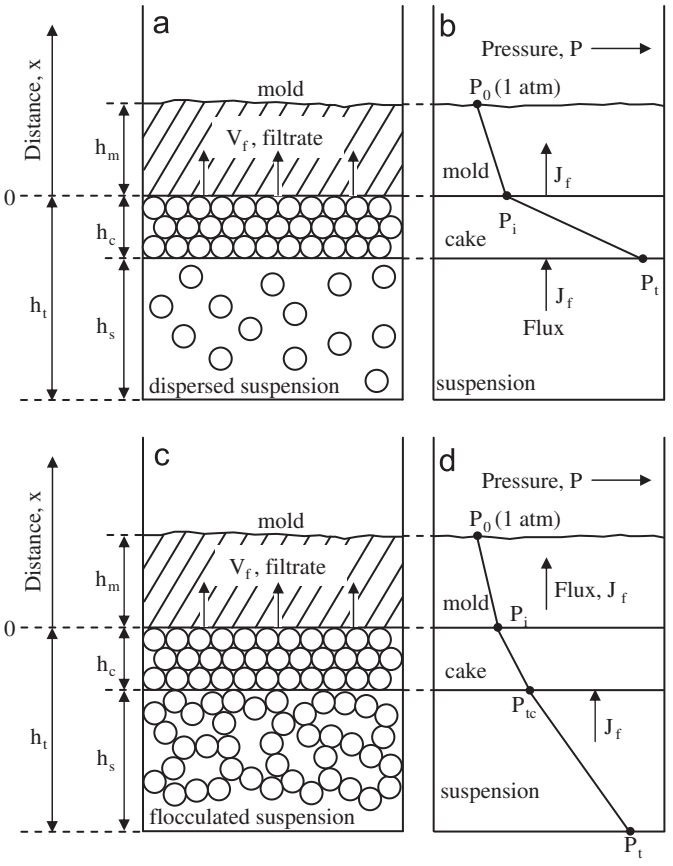

Fig. 2. Cross-sectional views of the filtration models (a, c) and hydraulic pressure across the consolidated layer and the mold (b, d) for well dispersed suspensions (a, b) and flocculated suspensions (c, d).

flocculated suspension and the hydraulic pressure profile across the mold, consolidated layer and flocculated suspension. The relation between suspension height and filtration time at a constant pressure, ΔP_s ($=P_t-P_i$), for an initially flocculated suspension is presented by Eq. (2) [5–7,10],

$$\Delta P_s t = \eta BS^2(H_0C_0)^2 \int_{H_0}^{h_s} \frac{h_s{}^2}{(h_s-H_0C_0)^3}\,dh_s$$
$$= \eta BS^2(H_0C_0)^2 \left\{ \frac{1}{2}\left[\frac{h_s{}^2}{(h_s-H_0C_0)^2} - \frac{H_0{}^2}{(H_0-H_0C_0)^2}\right] + \left[\frac{h_s}{(h_s-H_0C_0)} - \frac{H_0}{(H_0-H_0C_0)}\right] + \ln\left(\frac{H_0-H_0C_0}{h_s-H_0C_0}\right)\right\} \quad (2)$$

where BS^2 is treated as a constant value, B is the ratio of shape factor to the tortuosity constant, S is the ratio of the total solid surface area to the apparent volume. The specific filtration resistance (α_s) for a flocculated suspension in Fig. 2(c) is expressed by Eq. (3).

$$\alpha_s = BS^2(H_0C_0)^2 \frac{h_s}{(h_s-H_0C_0)^3} \quad (3)$$

In Eq. (1), the α_s value is treated as a constant value. On the other hand, Eq. (3) of the specific resistance is a function of filtration time because h_s changes with time. When S value in Eq. (3) is related to ε (the volume fraction of voids in the flocculated layer) and D (particle diameter) by Eq. (4), α_s value is expressed by Eq. (5), because $(1-\varepsilon)$ is equal to C_0H_0/h_s for a flocculated suspension.

$$S = \frac{6(1-\varepsilon)}{D} \quad (4)$$

$$\alpha_s = \left(\frac{36B}{D^2}\right)(H_0C_0)^4 \frac{1}{h_s(h_s-H_0C_0)^3} \quad (5)$$

The filtration process with a specific resistance by Eq. (5) is represented by Eq. (6).

$$\Delta P_s\, t = \int_{H_0}^{h_s} \eta\alpha_s h_s dh_s = \eta\left(\frac{36B}{D^2}\right)(H_0C_0)^4 \int_{H_0}^{h_s} \frac{1}{(h_s-H_0C_0)^3}\,dh_s$$
$$= \left(\frac{18B}{D^2}\right)\eta\,(H_0C_0)^4 \left[\frac{1}{(H_0-H_0C_0)^2} - \frac{1}{(h_s-H_0C_0)^2}\right] \quad (6)$$

The experimental specific resistance was determined by Eq. (7) [10,11] at the interval of $\Delta t=40$ seconds.

$$\alpha_s(\text{observed}) = \frac{(\Delta P_t/h_t)}{\eta(-\Delta h_t/\Delta t)} \quad (7)$$

Experimentally measured h_t–t relation at a constant ΔP_t was analyzed with Eqs. (1), (2) and (6). The measured specific resistance (Eq. (7)) was also compared with α_s values determined from Eqs. (1), (3) and (5). In this paper, aqueous alumina suspensions of 7 or 20 vol% solid were consolidated at 1–10 MPa.

4. Results and discussion

4.1. Zeta potential and rheology of colloidal alumina suspensions

Fig. 3 shows the zeta potential of alumina particles in a 0.001 M-NH_4NO_3 solution as a function of suspension pH [12]. The isoelectric point was pH 8.7. At a pH below the isoelectric point, the number of positively charged $AlOH_2^+$ sites becomes greater than that of negatively charged AlO^- sites. The zeta potential at pH 3.0 was +42 mV. The opposite case occurs at a pH above the isoelectric point. The zeta potential at pH 9.0 was −10 mV.

Fig. 4 shows typical shear rate–shear stress relations for alumina suspensions of 7–20 vol% solid at pH 3–9. According to our recent study [6], the critical surface potential of submicrometer-sized particles causing a colloidal phase transition (dispersed particles→flocculated particles) is calculated to be 18.2 mV for 100 nm diameter and 12.8 mV for 500 nm diameter at 1 atm. That is, the surface potential of alumina particles at pH 3.0 (Fig. 3) was higher than the critical surface potential. However, the surface potential at pH 9.0 (Fig. 3) was comparable to the critical surface potential for the phase transition, increasing the probability of flocculation due to the thermal

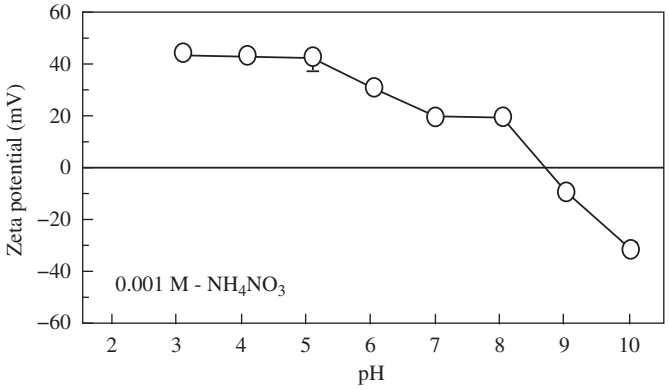

Fig. 3. Zeta potential of alumina particles as a function of suspension pH.

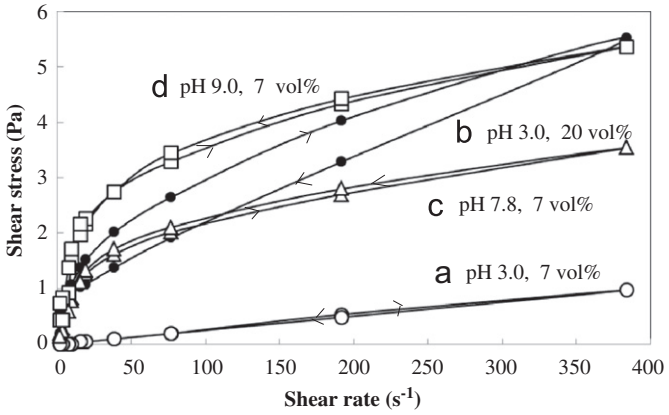

Fig. 4. Shear stress–shear rate relation for alumina suspensions at pH 3.0–9.0.

energy of alumina particles. As seen in Fig. 4, the acidic suspension at 7 vol% solid (pH 3) behaved as a Newtonian fluid with a low apparent viscosity, reflecting the high dispersion state of positively charged alumina particles. The increased solid content at pH 3 changed the shear rate–shear stress relation to a pseudoplastic behavior with hysteresis loss, suggesting the possibility of flocculation of dispersed particles. The distance (H) between two particles (diameter D) in a random close packing structure is expressed by Eq. (8) [4],

$$\frac{H}{D}=\left(\frac{1}{3\pi C_0}+\frac{5}{6}\right)^{1/2}-1 \tag{8}$$

where C_0 is the solid content of suspension. The H/D ratio is 0.168 for $C_0=0.2$ and approaches 0 at $C_0=0.637$. The increased solid content decreases drastically the H/D ratio, accelerating the touching of dispersed particles by the thermal energy and applied shear stress. The alumina suspensions at pH 7.8 and pH 9.0 showed also a pseudoplastic behavior at a low solid content of 7 vol%. This result is related to the formation of flocculated structure due to the low electrical repulsive energy. In this paper, the consolidation behavior during pressure filtration was analyzed for three types of suspensions of (b), (c) and (d) in Fig. 4, which showed a similar pseudoplastic behavior.

4.2. Kinetics of pressure filtration

Fig. 5 (a–c) show the relation between piston height (h_t) and filtration time for alumina suspensions at pH 3.0–9.0 during consolidation at 1 MPa. The h_t values decreased nonlinearly with time. The consolidation time is affected by the solid content and suspension pH. The measured piston height was analyzed by Eqs. (1), (2) and (6). The piston height of each alumina suspension was most fitted by Eq. (2) rather than Eq. (1) or Eq. (6), indicating the filtration of a flocculated suspension. In our previous papers [5–7], it was found that the critical pressure for the phase transition from dispersed to flocculated particles in 15 vol% alumina suspension at a constant crosshead speed of piston was 2.5 MPa at pH 3.0 (zeta potential, +48 mV) and 0.5 MPa at pH 7.8 (zeta potential, close to 0 mV), respectively. Therefore, the application of pressure above 0.5 MPa promotes the flocculation of alumina particles at pH 7.8 and 9.0 in addition to the weak repulsive energy (Fig. 3). The colloidal alumina particles in a dilute suspension (7 vol%) at pH 3.0 was expected to be dispersed under an atmospheric pressure. However, the h_t-t relation for 20 vol% solid suspension suggests the formation of flocculated particles at pH 3.0. This result is in accordance with the rheological property measured in Fig. 4. The shorter distance between two charged particles is one factor promoting the phase transition to a flocculated state under an applied pressure [7].

The consolidation time to reach the final height of colloidal cake became significantly longer in the suspension at pH 3.0 than at pH 7.8 or 9.0. This result is related to the increased specific resistance in the suspension at pH 3.0 as compared with the α_c values in the suspension at pH 7.8 or 9.0 (Fig. 5 (d–f)). The alumina particles at pH 3.0 are densely packed and the dehydration rate of the solution across the dense cake becomes lower. The alumina particles at pH 7.8 or 9.0 form a porous cake, which reduces the specific resistance of filtration and consolidation time.

Fig. 5 (d–f) show the relationship between filtration time and specific resistance of filtration for alumina suspensions during consolidation at 1 MPa. The measured α_s value increased gradually with increasing filtration time. At a longer filtration time approaching the final stage of consolidation, the observed α_s value increased rapidly with a

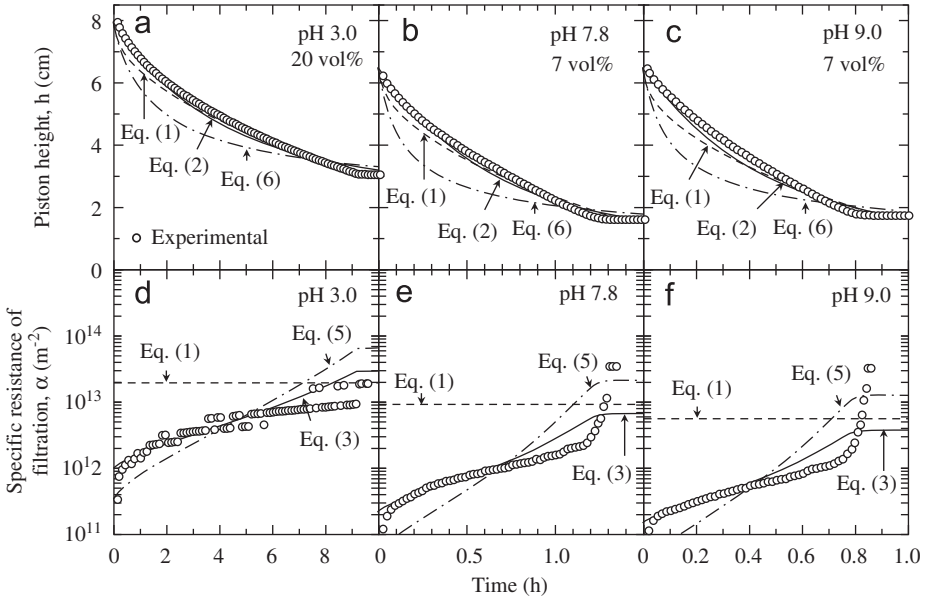

Fig. 5. Relation between filtration time and piston height (a–c) or specific resistance of filtration (d–f) for alumina suspensions at 1 MPa.

small increase in filtration time and reached a constant value. This result was not in accordance with the α_s calculated by Eq. (1) using the final packing density of alumina particles consolidated. On the other hand, Eqs. (3) and (5) can represent the time dependence of α_s using the measured h_t value. The simulation with Eq. (3) provided a good agreement of α_s values except for the final region of filtration. In Eq. (3), BS^2 value is treated as a constant value. However, the B and S values depend strongly on the structure of flocculated particles in the final stage of filtration. The actual flocculated particles form a dense structure in the final stage of filtration as compared with the structure defined by a constant BS^2 value. This discussion is supported by the larger α_s value by Eq. (5) whose S value increases with decreasing suspension height. That is, the difference of α_s values between the experiment and theory (Eq. (3)) becomes larger when the structure of flocculated particles changes to denser one in the final consolidation stage. Figs. 6 and 7 show the piston height and specific resistance of filtration at 4 and 10 MPa, respectively. The measured results in the suspensions at pH 3.0–9.0 were well fitted by Eq. (2) for the piston height and by Eq. (3) for the α_s value. This tendency was similar to the result observed in Fig. 5. Therefore, the filtration process of 310 nm-colloidal alumina particles at pH 3.0–9.0 in a wide applied pressure range of 1–10 MPa is well expressed by the filtration model for flocculated particles rather than a traditional filtration model for dispersed particles.

4.3. Properties of consolidated alumina compacts

Fig. 8 summarizes the influence of filtration pressure and suspension pH on the consolidation time of alumina suspension. Increase in filtration pressure shortens drastically the consolidation time of colloidal alumina suspensions. As seen in Eq. (2), the consolidation time is proportional to $1/\Delta P_s$ (applied pressure) for a same suspension height (h_s), explaining well the measured tendency. The consolidation time depends also upon BS^2 and C_0 values in Eq. (2), which are included in the specific filtration resistance in Eq. (3). The decrease of C_0 and BS^2 values leads to the short consolidation time. The BS^2 value reflects the microstructure of colloidal alumina cake and becomes larger in a denser microstructure [10]. The shorter consolidation time in the alumina suspension at pH 9.0 in Fig. 8 is related to smaller C_0 and BS^2 values. Fig. 9 shows the packing density of (a) wet and (b) calcined alumina compacts as a function of applied pressure of filtration. The packing density of alumina particles at pH 3.0 and 9.0 under compressive stress was not sensitive to the applied pressure. However, the packing density of colloidal alumina particles at pH 7.8 increased greatly with increasing applied pressure. The above result is closely related to the flexibility of the network of agglomerated alumina particles. After the calcination at 700 °C in air, the packing density of alumina compact was nearly independent of applied pressure and increased in the following order of suspension pH: pH 9 (50.2–52.6% relative density) < pH 7.8 (53.4–56.3% relative density) < pH 3.0 (59.7–61.1% relative density). The same order of suspension pH was also measured on the packing density of colloidal alumina particles consolidated in gypsum mold or pressure filtration at a constant crosshead speed of piston [13,14]. That is, the packing property of colloidal alumina particles is not affected by the applied pressure and controlled by the structure of network of alumina particles in the suspension. The positively charged alumina particles in an acidic suspension are densely packed during consolidation.

The difference in packing density of alumina particles between wet and calcined compacts represents the relaxation of packed colloidal alumina particles. The degree of relaxation increased in the following order of suspension

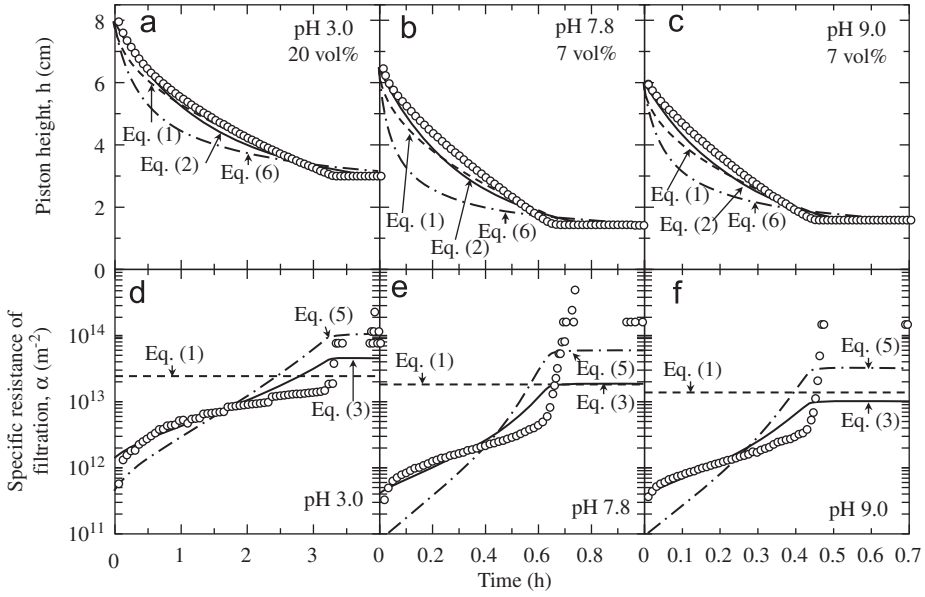

Fig. 6. Relation between filtration time and piston height (a–c) or specific resistance of filtration (d–f) for alumina suspensions at 4 MPa.

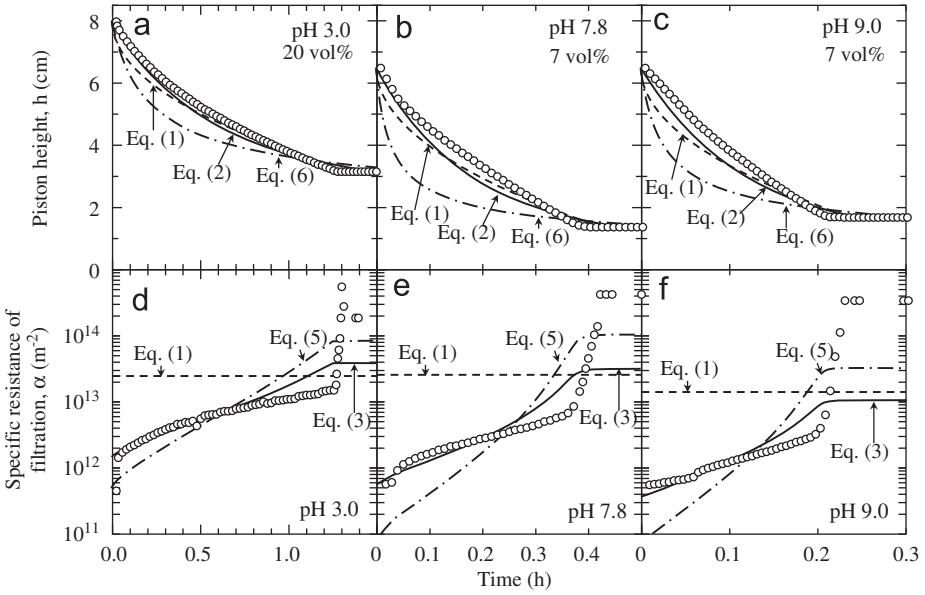

Fig. 7. Relation between filtration time and piston height (a–c) or specific resistance of filtration (d–f) for alumina suspension at 10 MPa.

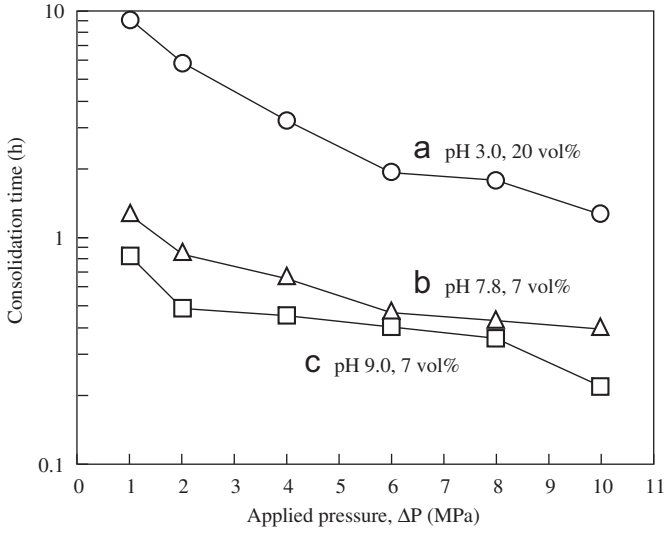

Fig. 8. Influence of filtration pressure on consolidation time of 310 nm-Al_2O_3 particles.

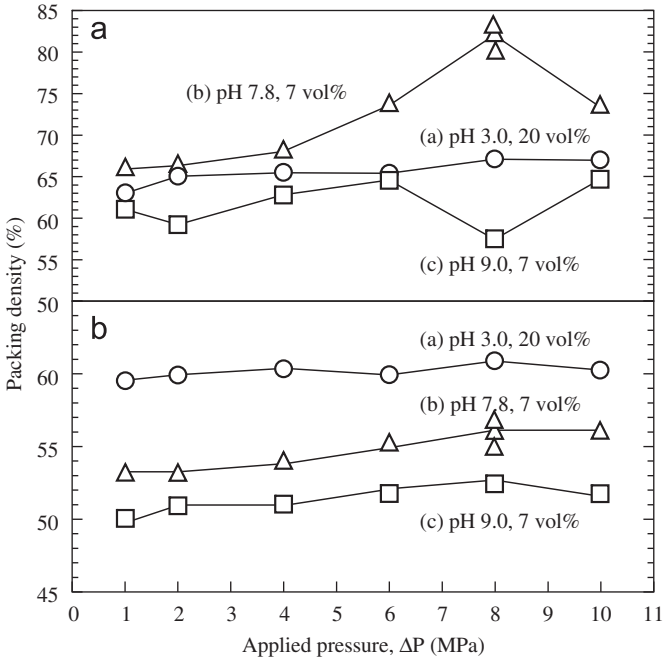

Fig. 9. Influence of filtration pressure on packing density of (a) wet and (b) calcined alumina compacts.

pH: pH 3.0 < pH 9.0 < pH 7.8. In our previous paper [15], the viscoelastic properties of flocculated alumina suspensions were analyzed by Maxwell and Voigt models. The flocculated suspension behaves as a liquid like at a low particle concentration and the influence of solid element of the Voigt model becomes stronger with increasing solid content. The large difference in packing density between Fig. 9(a) and (b) reflects the small Young's modulus of solid element in a wet alumina compact. The compressive strain under an applied stress is large for a small Young's modulus, causing a large amount of relaxation after the elimination of applied pressure.

Fig. 10 shows the microstructures of alumina compacts after calcination at 700 °C in air. The alumina compacts with 0.7–2.6 cm height were cut at three parts (top, middle and bottom) along the direction of height. No significant difference was observed in the microstructures along the direction of height. The microstructures of alumina compacts formed at 1 MPa of applied pressure became denser in the order of (e) (pH 9.0) < (c) (pH 7.8) < (a) (pH 3.0). This tendency is well understood by the packing density measured in Fig. 9(b). The increase of filtration pressure to 10 MPa provided little change in the microstructures of alumina compacts formed at each suspension pH ((b), (d) and (f)). The microstructure of calcined alumina compact is mainly dominated by the surface property of colloidal

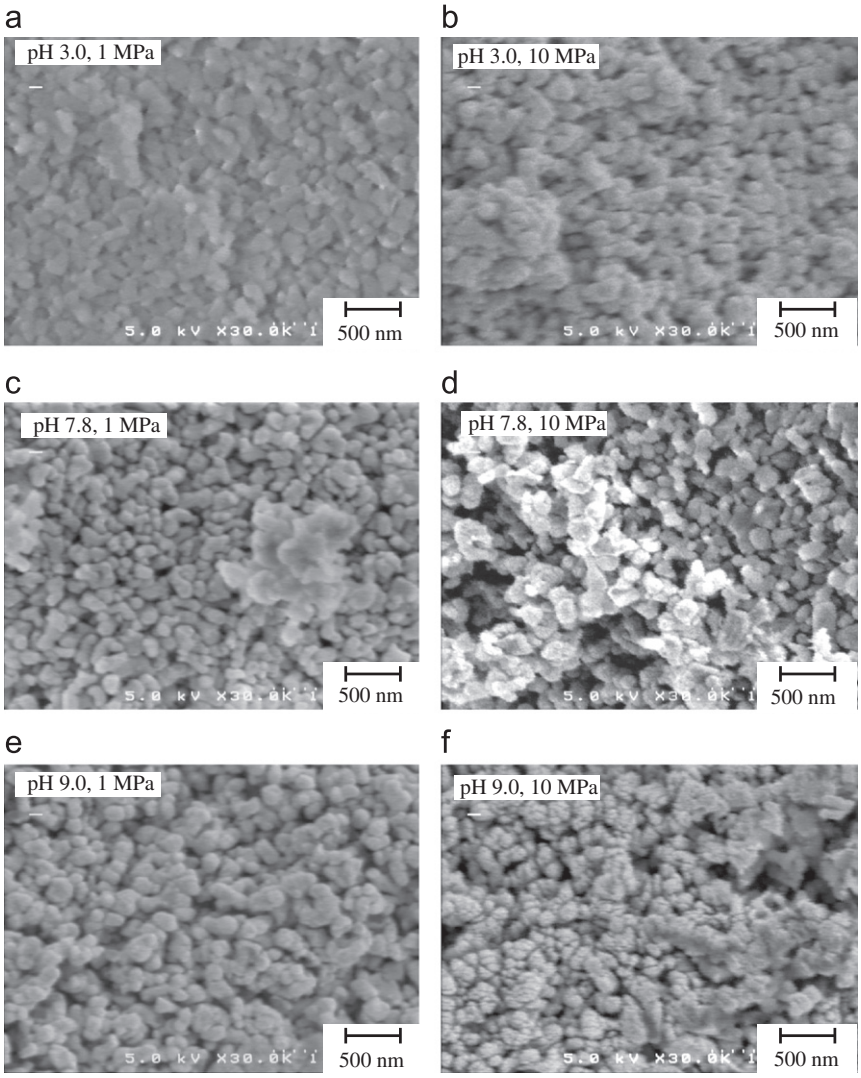

Fig. 10. Microstructures of alumina compacts consolidated at 1 or 10 MPa and calcined at 700 °C.

alumina particles in a solution and nearly independent of applied pressure during consolidation.

5. Conclusions

The dispersibility of 310 nm-colloidal alumina particles were associated with their surface potential, the solid concentration in a suspension and the pressure applied as a shear stress or during pressure filtration. The filtration process of 310 nm-colloidal alumina particles at pH 3.0–9.0 in a wide applied pressure range of 1–10 MPa was well expressed by the filtration model for flocculated particles. The measured specific resistance of filtration increased gradually with increasing filtration time. An increase of applied pressure, a decrease of particle concentration and a porous microstructure of colloidal alumina cake resulted in the short consolidation time. The pressure dependence of packing density of wet alumina compact under a compressive stress became large for the colloidal alumina particles at near isoelectric point. However, the packing density of alumina compact after calcination was independent of filtration pressure and increased in the following order of colloidal alumina particles: negatively charged particles (in basic suspension) < positively charged particles at near isoelectric point < positively charged particles (in acidic suspension). The packing property of colloidal alumina particles is controlled by the structure of network of alumina particles in a solution. The difference in packing density between wet and calcined compacts reflects the relaxation of colloidal alumina particles packed under a compressive stress.

References

[1] F.F. Lange, K.T. Miller, Pressure filtration: kinetics and mechanics, American Ceramic Society Bulletin 66 (1987) 1498–1504.
[2] I.A. Aksay, C.H. Schilling, Advances in Ceramics, Forming of Ceramics, vol. 9, in: J.A. Mangels, G.L. Messing (Eds.), The American Ceramic Society, Columbus, Ohio 1984, pp. 85–93.
[3] A. Dietrich, A. Neubraund, Y. Hirata, Filtration behavior of nanoparticulate ceria slurries, Journal of the American Ceramic Society 85 (2002) 2719–2724.

[4] Y. Hirata, M. Nakamura, M. Miyamoto, Y. Tanaka, X.H. Wang, Colloidal consolidation of ceramic nanoparticle by pressure filtration, Journal of the American Ceramic Society 89 (2006) 1883–1889.
[5] Y. Hirata, Y. Tanaka, Pressure filtration model of ceramic nanoparticles, Journal of the American Ceramic Society 91 (2008) 819–824.
[6] Y. Hirata, N. Matsunaga, S. Sameshima, Phase transition and consolidation of colloidal nanoparticles, Ceramic Transactions 223 (2010) 101–112.
[7] Y. Hirata, K. Matsushima, S. Baba, N. Matsunaga, S. Sameshima, Theoretical and experimental analyses of colloidal processing of nanoparticles, Advances in Science and Technology 62 (2010) 131–140.
[8] Y. Hirata, H. Uchima, Y. Tanaka, N. Matsunaga, The effect of electric field on pressure filtration of ceramic suspensions, Journal of the American Ceramic Society 92 (2009) S57–S62.
[9] K. Matsushima, Y. Hirata, N. Matsunaga, S. Sameshima, Pressure filtration of alumina suspensions under alternating current field, Colloids and Surfaces A: Physicochemical and Engineering Aspects 364 (2010) 138–144.
[10] Y. Tanaka, Y. Hirata, N. Matsunaga, M. Nakamura, S. Sameshima, T. Yoshidome, Pressure filtration of nanometer-sized SiC powder, Journal of the Ceramic Society of Japan 115 (2007) 786–791.
[11] N. Matsunaga, A. Yamashita, Y. Hirata, Consolidation behavior of nanometer-sized SiC particles with phenylalanine through pressure filtration at 1 MPa, Journal of the Ceramic Society of Japan 119 (2011) 161–167.
[12] S. Baba, Y. Hirata, N. Matsunaga, S. Sameshima, The effect of an amino acid of low molecular weight on consolidation of nanoparticle suspensions. Journal of Ceramic Processing Research, in press.
[13] Y. Hirata, Y. Tanaka, Y. Sakamoto, Packing density and consolidation energy of colloidal particles through pressure filtration, Advances in Science and Technology 45 (2006) 471–479.
[14] Y. Hirata, X.H. Wang, Y. Hatate, K. Ijichi, Electrical properties, rheology and packing density of colloidal alumina particles, Journal of the Ceramic Society of Japan 111 (2003) 232–237.
[15] Y. Hirata, K. Matsushima, N. Matsunaga, S. Sameshima, Viscoelastic properties of flocculated alumina suspensions during pressure filtration, Journal of the Ceramic Society of Japan 118 (2010) 977–982.